SUPPLEMENTAL MATERIAL

Moving while you're stuck: A macroscopic demonstration of an active system inspired by binding-mediated transport in biology

Kanghyeon Koo,[1] Shankar Lalitha Sridhar,[2] Noel Clark,[3] Franck Vernerey,[2,*] and Loren Hough[3,†]

[1] *Civil, Environmental and Architectural Engineering, University of Colorado Boulder, Boulder, Colorado-80309, USA*
[2] *Department of Mechanical Engineering, University of Colorado Boulder, Boulder, Colorado-80309, USA*
[3] *Department of Physics and BioFrontiers Institute, University of Colorado Boulder, Boulder, Colorado-80309, USA*

EXPERIMENT

Design and Setup

This section describes the design and detailed information on the components of the macroscopic experimental system used in this study. We describe the build-up of the components of the setup from the bottom up, see Fig.1. An isolation frame is mounted on an optical table to support a Quinn Acoustics 10" subwoofer. We generated Gaussian white noise with a sampling frequency of 1.5kHz using Matlab functions. The digital signal was converted to analogue using a Digital-to-analog converter (DAC), and the signal was then fed to a power amplifier (Fig.2). We measured the average voltage after the amplifier with a multimeter. Our experiments were performed using signals between 12 and 22 VAC. The isolation frame serves to prevent lateral vibration and elevated the speaker above the table. Onto the speaker, we glued a spool(PolyLite PLA, diameter 200 mm and height 52 mm) fit precisely into the rubber edge ring of the speaker. The spool served as a platform for us to mount another sheet of acrylic, the roof (2.2 mm thickness). This acrylic sheet held the strings holding the magnetic heads as well as 3D-printed walls to keep adjacent strings

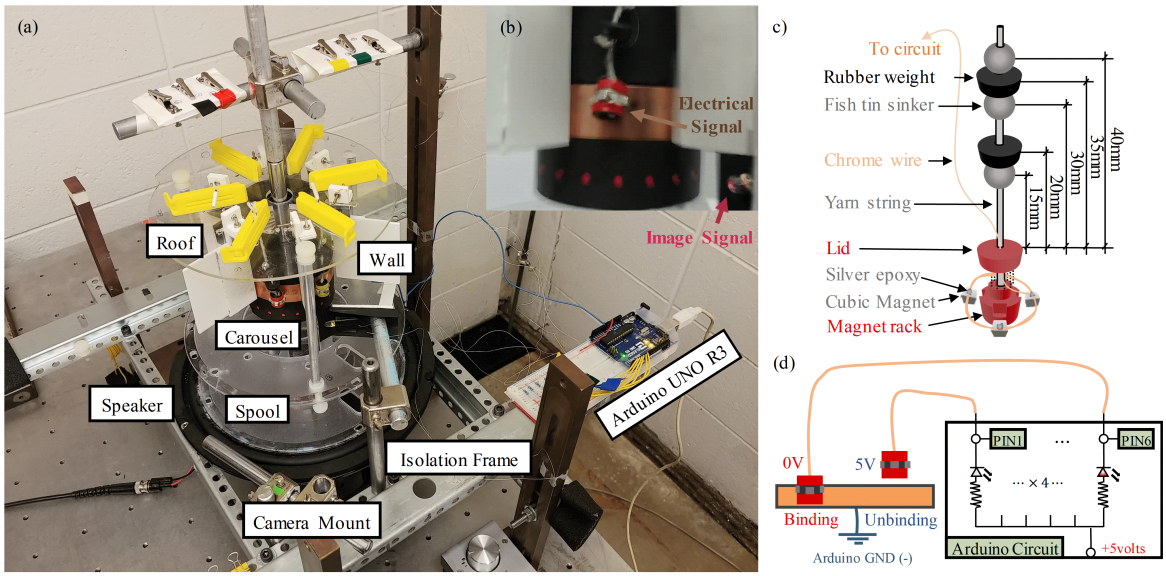

FIG. 1: (a) The overview picture of the experimental setup (without camera deck) (b) Data from one frame of video: a positions speed markers(red dot) for rotation angles, a position of the string head(red two strips), and an image on-off signal(red light diode. (c) the detail and component of tether design. (d) The illustration of circuit how to catch bindings or unbinding events as electrical signals.

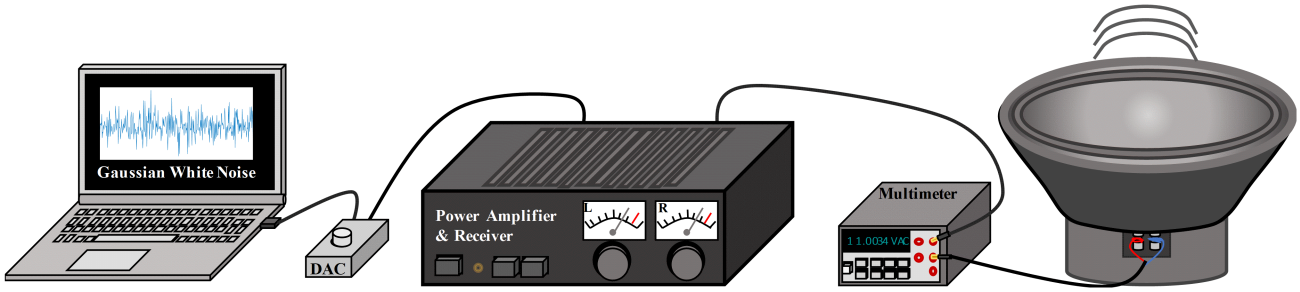

FIG. 2: The process by which an audio system send digital Gaussian white noise to speakers, and monitoring system for its amplitudes.

from getting tangled.

The rotating carousel was suspended on a frame built above the speaker assembly. As a result, the carousel was isolated from the speaker vibrations. Fig 1b in the main text shows the details of the carousel design. The carousel consists of a 3D printed plate (77mm diameter) with a ball bearing glued into its center. The ball bearing (NMB Technologies, 1mm diam balls and 16.8mm outer diameter) is suspended by a metal shaft along its axis to allow relatively free rotation. We place 36 equally spaced circular magnets of diameter 6mm on the rim of the inner acrylic round plate touching as to mimic as much as possible a continuous binding surface. The magnets act as the binding sites. The circular geometry allows for continuous tracking of the rotation angle. The acrylic plate was covered with black paper, reinforced with cardboard disks. The black paper provided a barrier for the magnetic heads and facilitated image processing by providing good contrast with the magnetic heads. We used a series of red dots as a speed strip to be able to determine the rotation angle of the carousel. A copper strip covering the location of the magnets provided a ground for electrical measurement of the binding.

The magnetic heads were made from 3-D printed(Ninja Flex) cylindrical head of height 11mm and diameter 10.5mm that are loaded with four cubic magnets each of size 3mm. The magnetic head was attached to the acrylic roof by a 60 mm long piece of yarn. Supplmental Fig. 1c illustrates the string head construction and how the string head is connected to the roof. Three tin fishing sinkers(Water Gremlin Green) and two Ninja flex weights are clamped on the yarn to induce randomness and avoid resonance during vibration, and each location is indicated in the Fig 1c. Each string is attached to the roof by clips (yellow), which allows us to easily change the number of strings. The strings are physically separated from each other by 3D printed plastic walls to prevent them from sticking to each other. Fig 1a shows a setup with six equally spaced strings which were removed as necessary for fewer strings. We used an electrical connection between magnetic head and a copper strip to detect binding. A thin, flexible wire attached to the magnetic head provided an electrical connection to detect binding. We used high strength and thin flexible and conductive chrome wire (Medwire, 0.17mm diameter) to prevent cutting arising from fatigue and minimize the interference of the wire when the string oscillates. The four magnets and the chrome wire are connected with silver epoxy (MG Chemicals), which makes the head unit light and easy to assemble.

We recorded video of the position of the carousel and one of the strings, which we assumed to be representative. The other strings were not visible in our frame of view. We combined video and electrical recordings to measure the binding and unbinding rate, the positions of binding and unbinding, and the rotation of the carousel. To obtain the sampling data for binding and unbinding events, we connect the magnetic head of the string and the circular magnetic sites to an Arduino UNO R3 microcontroller that is connected to a computer. The electrical circuit is closed whenever the magnetic head makes contact with the carousel, and this data is recorded by the microcontroller which acts as a switch, see Fig. 1d. A thin and smooth copper strip of width 19mm is glued to the outer surface of the carousel and the middle of the pack of round magnets to help reduce noise in the signals from imperfect contact. We track the magnetic head of the vibrating string along the surface of the carousel using a video-camera to obtain its position relative to the rest position at the time of binding or unbinding. Each experiment is run for 15 min, and a video camera (LG V30) is used to record the rotation of the carousel at a frame rate of 120 FPS. Circular patches painted at the bottom of the carousel help in tracking the angle of rotation during the post-processing of the video. We developed the code using the OpenCV python library to track these two motions. This library makes it easy to find the center of the string head in red. The rotation angle can be tracked simply by comparing the distance between a speed marker point closest to center in the current configuration and the speed markers in previous configuration. Hence, our macroscopic experimental setup gives us all the data we desire.

The electrical signal used to measure binding and unbinding events contained significant noise, primarily from

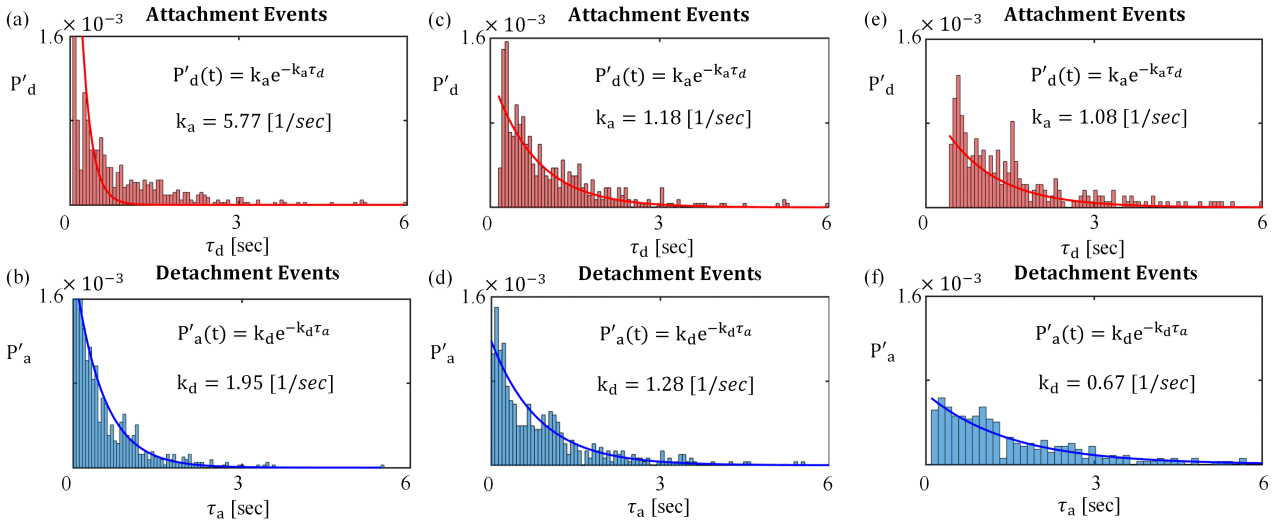

FIG. 3: A test of our choice of time cuttofs for the shortest unbinding events Δt_{cr_1} and that the shortest binding events were Δt_{cr_2}. (a) and (b) Probability histograms of the lifetimes of bound and free states when $\Delta t_{cr_1} = 0.05s$ and $\Delta t_{cr_2} = 0.005s$. (c) and (d) Probability histograms of the lifetimes of bound and free states when $\Delta t_{cr_1} = 0.15s$ and $\Delta t_{cr_2} = 0.015s$. (e) and (f) Probability histograms of the lifetimes of bound and free states when $\Delta t_{cr_1} = 0.45s$ and $\Delta t_{cr_2} = 0.045s$. We concluded that the choices derived from the videos (c) and (d), $\Delta t_{cr_1} = 0.15s$ and $\Delta t_{cr_2} = 0.015s$ determined primarily from visual inspection of the videos were the most accurate and used those for analysis of the data. Significantly shortening these times introduced artifactual peaks, whereas making them much longer excluded data.

collisions of the magnetic particle with the copper strip that did not result in binding. We compared video recordings frame-by-frame with the electrical signal, and determined that the shortest unbinding unbinding events were $\Delta t_{cr_1} = 0.15s$, and that the shortest binding events were $\Delta t_{cr_2} = 0.015s$. We tested whether the choice of these parameters significantly affected the resulting calculated rates. The accuracy of this choice was particularly apparent for k_a, where decreasing these time resulted in significantly poorer fits to the data and that lengthening it gave somewhat worse fits but did not significantly change the fit value (Fig. 3). This is as expected for fits to noisy exponential curves with extra noise occurring at short times. Including the short time noise will change the fit value, and excluding too much good data will reduce the signal to noise.

Detailed data

* franck.vernerey@colorado.edu
† loren.hough@colorado.edu

TABLE I: Detailed results of all 18 data sets of the experiment. $\bar{k}_a$ and $\bar{k}_d$ are the average values of k_a and k_d and $\sigma_{\bar{p}}$ and $\sigma_{\bar{D}^*}$ are the errors propagated from the fit errors of the underlying measurements used to calculate p and D^* respectively.

Fig. 4	N	$D[\theta^2/sec]$	$\bar{k}_a[1/sec]$	$\bar{k}_d[1/sec]$	$\sigma[\theta]$	$p = \bar{k}_a/(\bar{k}_a + \bar{k}_d)$	$D^* = 2D/\sigma^2(\bar{k}_a + \bar{k}_d)$	$\sigma_{\bar{p}}$	$\sigma_{\bar{D}^*}$
a	1	0.704	0.066	2.700	6.640	0.976	0.012	0.774×10^{-2}	0.354×10^{-2}
b	1	19.727	1.182	1.281	7.687	0.520	0.271	2.121×10^{-2}	1.174×10^{-2}
c	1	12.460	1.955	0.302	9.606	0.134	0.121	0.917×10^{-2}	0.477×10^{-2}
d	1	1.605	0.043	2.938	6.333	0.986	0.027	0.501×10^{-2}	0.900×10^{-2}
e	1	27.846	0.557	1.391	10.596	0.714	0.256	2.760×10^{-2}	2.370×10^{-2}
f	1	14.567	3.624	0.253	13.309	0.065	0.042	0.422×10^{-2}	0.089×10^{-2}
g	3	7.605	1.841	0.277	8.435	0.869	0.101	1.395×10^{-2}	0.982×10^{-2}
h	3	39.650	0.667	1.461	9.212	0.313	0.439	2.165×10^{-2}	1.656×10^{-2}
i	3	57.220	0.176	6.001	9.522	0.029	0.204	0.212×10^{-2}	0.985×10^{-2}
j	3	7.545	2.642	0.127	11.488	0.954	0.041	0.906×10^{-2}	0.765×10^{-2}
k	3	29.110	1.083	0.571	12.043	0.655	0.243	2.606×10^{-2}	1.574×10^{-2}
m	3	50.046	0.392	1.813	12.433	0.178	0.294	1.062×10^{-2}	1.033×10^{-2}
n	6	8.666	2.878	0.812	8.616	0.780	0.063	5.183×10^{-2}	1.436×10^{-2}
o	6	62.179	0.786	1.931	8.782	0.289	0.593	1.684×10^{-2}	2.280×10^{-2}
p	6	106.499	0.177	7.496	9.660	0.023	0.297	0.239×10^{-2}	2.290×10^{-2}
g	6	1.748	2.474	0.053	9.945	0.979	0.014	1.371×10^{-2}	0.896×10^{-2}
r	6	10.712	1.187	0.532	10.473	0.690	0.114	4.365×10^{-2}	1.544×10^{-2}
s	6	92.985	0.448	2.665	12.422	0.144	0.387	0.900×10^{-2}	1.354×10^{-2}

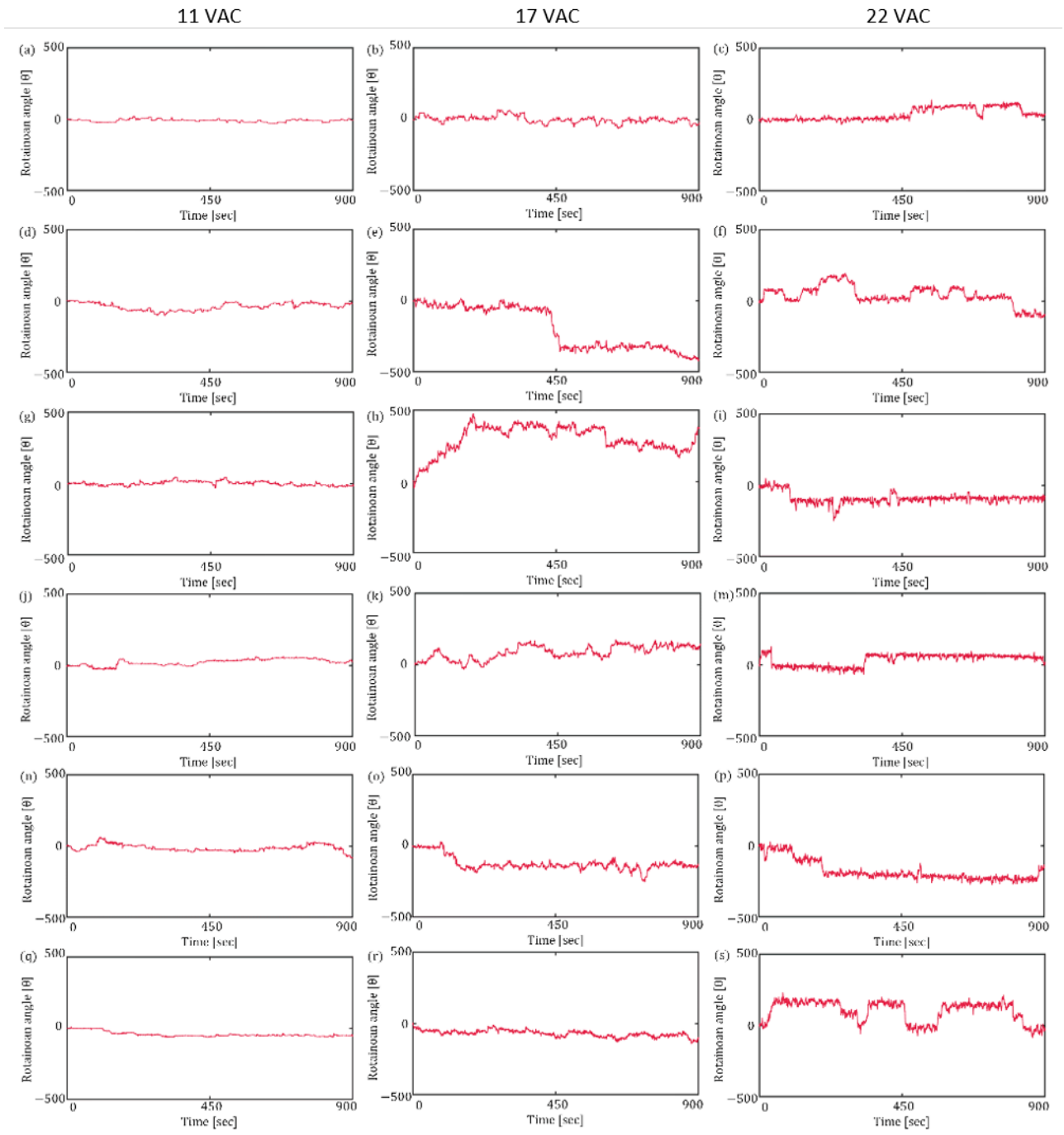

[t]

FIG. 4: Trajectories for all 18 conditions of the diffusion experiments.